Continuous tuning of W-doped VO_2 optical properties for terahertz analog applications

G. Karaoglan-Bebek,[1] M. N. F. Hoque,[2] M. Holtz,[3] Z. Fan,[2] and A. A. Bernussi[2,a)]
[1]*Department of Physics and Nano Tech Center, Texas Tech University, Lubbock, Texas 79409, USA*
[2]*Department of Electrical and Computer Engineering and Nano Tech Center, Texas Tech University, Lubbock, Texas 79409, USA*
[3]*Department of Physics, Texas State University, San Marcos, Texas 78666, USA*

(Received 4 October 2014; accepted 6 November 2014; published online 17 November 2014)

Vanadium dioxide (VO_2), with its characteristic metal-insulator phase transition, is a prospective active candidate to realize tunable optical devices operating at terahertz (THz) frequencies. However, the abrupt phase transition restricts its practical use in analog-like continuous applications. Incorporation of tungsten is a feasible approach to alter the phase transition properties of thin VO_2 films. We show that amplitude THz modulation depth of ∼65%, characteristic phase transition temperature of ∼40 °C, and tuning range larger than 35 °C can be achieved with W-doped VO_2 films grown on sapphire substrates. W-doped VO_2 films can also be used to suppress Fabry-Perot resonances at THz frequencies but at temperatures much lower than that observed for undoped VO_2 films. The gradual phase transition temperature window allows for precise control of the W-doped VO_2 optical properties for future analog based THz devices. © *2014 AIP Publishing LLC*.
[http://dx.doi.org/10.1063/1.4902056]

Vanadium dioxide (VO_2) has been receiving considerable attention due to its prospective use as a tunable material in a variety of optical components. VO_2 exhibits a well-known reversible metal-insulator transition (MIT), which is accompanied by change in the electrical conductivity by several orders of magnitude.[1–3] Tunable optical components are fundamental to realize smart windows, frequency selective filters, ultrafast switches, and spatial light modulators.[3–5] For photon energies below the bandgap, VO_2 exhibits high optical transmittance in the insulating phase and low optical transmittance in the metallic phase, leading to a stark optical contrast. This is particularly important at terahertz (THz) frequencies where transmission amplitude modulation depths as large as 85% has been recently reported for thin film VO_2.[6] This characteristic has motivated intensive investigations of VO_2 based active optical components for THz applications.[7–9]

Although considerable progress has been made using VO_2 as the tunable material in active devices, inherent limitations prevent further development of VO_2 based devices for analog applications. The metal-insulator phase transition temperature of undoped VO_2 ($T_{MIT} \sim 68\,°C$) is abrupt, with window of ∼1–2 °C. This digital-like on/off abruptness is problematic for applications that demand analog-like operation mode such as continuously tunable spatial light modulators or optical switches. For thermally controlled active optical components, the high T_{MIT} above ambient leads to sluggish device response when switching between the insulating and the metallic phases, resulting in slow speed operation. Thus, for ease of control and analog attributes, it is critical to engineer the MIT characteristics of the VO_2 to achieve both lower T_{MIT} and, most importantly, a large transition temperature window in which optical properties can be continuously tuned.

Chemical doping has been confirmed to be effective in modifying T_{MIT} while retaining the desired contrast in electrical and optical properties exhibited by VO_2. In addition, doping can prospectively be used to modify the response time of VO_2.[10,11] It has been shown that T_{MIT} can be reduced by doping VO_2 with W,[12–21] Cu,[22] Mo,[23] Nb,[24] and Fe,[25] or the T_{MIT} can be increased using Ti (Refs. 13 and 26) as the dopant. Among the dopants used to reduce the T_{MIT}, tungsten has attracted particular attention. By varying the W dopant concentration over a few percent, T_{MIT} of VO_2 can be controlled between room temperature and 68 °C.[12–20] This change in T_{MIT} is accompanied by variations in electrical conductivity and optical properties.[12,20] This is very promising for active optical components, particularly in the THz range. Although there have been many reports on THz studies of undoped VO_2, corresponding investigations of W-doped VO_2 remain largely unexplored.[18] In particular, we are aware of no reports on gradually and continuous tuning the optical properties of VO_2 over a large temperature window at THz frequencies.

In this paper, we report THz studies of W-doped VO_2 thin films grown on sapphire substrates. We reduced the phase transition temperature to ∼40 °C with a transition width of ∼35 °C. We show that the refractive index of W-doped VO_2 can be continuously tuned within the MIT and this allows for precise control of the transmission properties of the VO_2 films. Both the real and the imaginary parts of the refractive index can be tuned from ∼20 to 50 in the temperature range 35–80 °C. Changes in THz amplitude modulation, refractive index, and T_{MIT} with the incorporation of tungsten dopants are found to correlate with variations in the electrical properties of these films. We show that the width and the sharpness of the MIT and the antireflection condition at THz frequencies of W-doped VO_2 films can be controlled by varying the tungsten concentration.

[a)]Author to whom correspondence should be addressed. Electronic mail: ayrton.bernussi@ttu.edu

 © 2014 AIP Publishing LLC

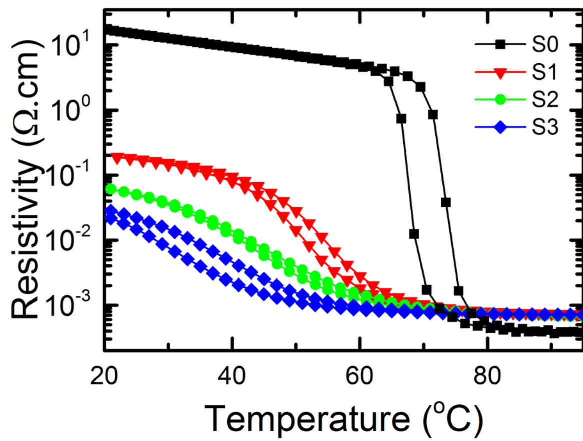

FIG. 1. Temperature dependent resistivity measurements for samples S0, S1, S2, and S3 during the heating and cooling cycles.

Undoped and W-doped VO_2 films ~150 nm in thickness were prepared by reactive DC magnetron sputtering deposition technique on c-plane (0001) oriented sapphire substrates. Sapphire is chosen as the substrate due to its high transparency in the THz range. One undoped, denoted as S0, and three W-doped VO_2 samples, denoted as S1, S2, and S3, were investigated. Details of the sample fabrication can be found in Ref. 27. Tungsten incorporation in the VO_2 films was realized by co-sputtering a tungsten wire (99.95% purity) during the film deposition. The W/V average atomic fraction was determined by X-ray photoelectron spectroscopy (XPS) and values of 1.47, 1.59, and 1.73 at. % for samples S1, S2, and S3, respectively. The resistivity of each sample during the heating and cooling cycles was determined by van der Pauw method.[27] X-ray diffraction measurements (not shown here) at room temperature revealed diffraction patterns characteristic of the monoclinic phase for all samples investigated; this result is consistent with what is expected for VO_2. THz transmission experiments were performed on the undoped and all W-doped VO_2 films at normal incidence in the 0.1–1.5 THz range using a commercial system.[6] The samples were placed in a hollow controlled thermoelectric heater/cooler stage for varying the temperature.

Figure 1 shows the temperature dependent resistivity measured for each sample during the heating and cooling cycles. We observe a systematic decrease in T_{MIT} and transition broadening with increasing W content. Sample S3 exhibits the largest deviation from undoped material, with $T_{MIT} \sim 40\,°C$ during the temperature rise cycle and transition width of $>35\,°C$. The significant reduction of T_{MIT} and increased transition width observed for the W-doped VO_2 samples shown in Fig. 1 are consistent with previous reports.[12–21] Variations in T_{MIT} and width of the phase transition among the investigated samples are readily attributed to the tungsten concentration. Previous reports indicate that the transition temperature of W-doped VO_2 can decrease at a rate of 22–25 °C/at. % W,[14–17] with increasing tungsten content. Using the determined T_{MIT} and W concentrations from XPS measurements, and including the T_{MIT} for undoped VO_2 from THz measurements, we determined a decrease rate of $\sim 22 \pm 4\,°C$/at. % W for the samples investigated in this work. Furthermore, our results show that the resistivity of W-doped VO_2 in the insulating (metallic) state is lower (higher) when compared to the resistivity of undoped VO_2 in the same phase. This characteristic is expected to result in different THz transmission properties as we will discuss below.

Figure 2 shows the THz transmission time waveforms and corresponding frequency spectra of one representative W-doped VO_2 film (sample S3) obtained at insulator, transition, and metallic states. Both the main transmitted pulse and the first round-trip reflected pulses at the air-VO_2/sapphire interface were observed at temperatures below and above the MIT (see Fig. 2). In the insulator state, the two pulses are in phase with each other. In the metallic state, a relative phase change of π is observed in the reflected pulse in Fig. 2(a), confirming the metallic phase at high temperatures. It is also evident that the time waveform amplitude of S3 decreases as the VO_2 film undergoes the phase transition from insulator to metallic state. The main THz transmitted pulse peak-to-peak amplitude ratio of insulator to metallic phase was determined as ~3.0 for sample S3. Above the T_{MIT} (at $T = 80\,°C$), we determined resistivity of $7 \times 10^{-4}\,\Omega$ cm for sample S3. The low resistivity of sample S3 heralds elevated free-carrier concentration. This, in turn, is responsible for the lower THz transmission at high temperatures ($T > T_{MIT}$).

An important parameter used in switching and modulation applications is the field amplitude modulation depth defined as

$$MD = (E_{low} - E_{high})/E_{low}, \tag{1}$$

where E_{low} and E_{high} are the THz field amplitudes below (20 °C) and above (80 °C) T_{MIT}. We determined MD = 74%,

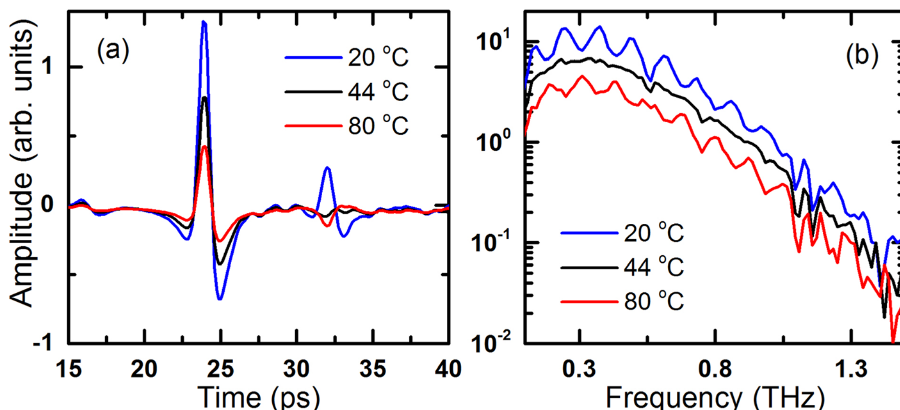

FIG. 2. THz transmission response of W-doped VO_2/sapphire sample S3 at temperatures below, within, and above the MIT. (a) THz time domain waveform and (b) corresponding frequency spectra.

64%, 67%, and 65% for samples S0, S1, S2, and S3, respectively. The observed variations in MD are attributed to differences in the resistivity of the investigated W-VO_2 samples when compared to undoped VO_2 films (see Fig. 1).

We observed that the THz transmission amplitude in all investigated films (not shown here) is consistent below T_{MIT}. On the other hand, when in the metallic phase, the transmission amplitude of W-doped VO_2 films is larger than that of undoped VO_2 samples. These observations are supported by the resistivity measurements, as shown in Fig. 1. We measured resistivity of 0.20, 0.06, and 0.08 Ω cm at the insulating state and 7.2×10^{-4}, 6.6×10^{-4}, and 7.1×10^{-4} Ω cm at the metallic state for samples S1, S2, and S3, respectively. In the case of the undoped VO_2 sample, resistivity of 17.58 Ω cm and 3.66×10^{-4} Ω cm for $T \ll T_{MIT}$ and $T \gg T_{MIT}$, respectively, were determined. Therefore, W-doped VO_2 films investigated here are more conductive at low temperatures but less conductive at high temperatures, when compared to undoped VO_2 samples. The corresponding THz frequency spectra, shown in Fig. 2(b) for sample S3, reveal the characteristic Fabry–Perot resonances for temperatures below and above the T_{MIT}. These are due to multiple reflections at the air-VO_2/sapphire interface.[6] The corresponding π phase shift of the resonance peaks is also evident in these two spectra. In contrast, for temperatures within the MIT (44 °C shown for sample S3), the reflected pulses in the THz time waveform (Fig. 2(a)) and the resonance peaks in the THz frequency spectra (Fig. 2(b)) were suppressed. This effect was previously reported for undoped VO_2 films, and it was attributed to the anti-reflecting (AR) condition which occurs at a specific electrical resistivity of the film as the temperature is varied.[6] This result confirms that thin W-doped VO_2 films can also function as an AR coating material at THz frequencies, but at much lower temperatures.

THz digital switching and modulation applications require sharp MIT and this can be achieved with undoped VO_2 films.[28,29] However, THz analog modulation and AR coating applications require broader and less abrupt MIT where the amplitude can be tuned over a wide range of temperatures. This can be realized with W-doped VO_2 which reduces the T_{MIT} and concurrently broadens the phase transition. This allows for precise control of the electrical and optical properties of VO_2 for THz optical device applications. To explore this attribute, we show in Fig. 3 the temperature-dependent THz transmitted field amplitude normalized to that of the bare sapphire substrate for samples S0, S1, S2, and S3. The expected thermal hysteresis loop is observed for all four cases. For samples S0, S1, S2, and S3 we determined, respectively, $T_{MIT} = 75.5$, 60.3, 56.1, and 41.1 °C from Fig. 3 (during the heating cycle). The T_{MIT} values for W-doped samples are considerably lower than that obtained for undoped VO_2. It is evident from the THz data shown in Fig. 3 that the tungsten incorporation into the VO_2 films changes considerably the phase transition properties, in good agreement with the observed temperature dependent resistivity results shown in Fig. 1. For instance, the THz transmission amplitude of sample S3 varies across the 30–65 °C range. This range is over an order of magnitude broader than that observed using THz measurements for the undoped VO_2 during the MIT.

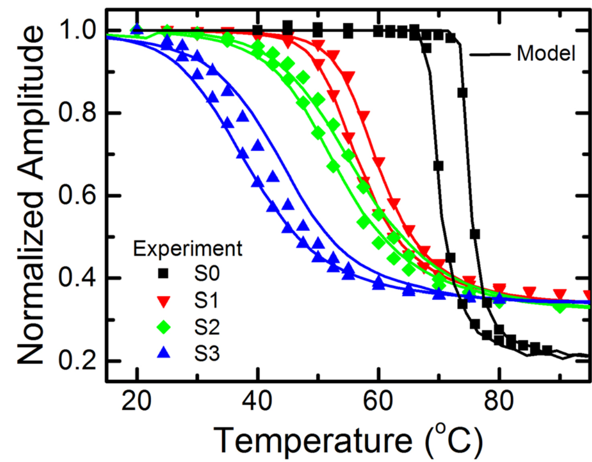

FIG. 3. Normalized THz transmission amplitude ratio (symbols) as a function of temperature for samples S0, S1, S2, and S3. Simulated THz amplitude ratio (solid line) using Eq. (2) and measured DC resistivity for each sample.

The optical constants of W-doped VO_2 can be determined from the changes in THz relative amplitude with the temperature. The ratio of the complex field amplitude $(\tilde{E}_{f+s}(\omega))$ transmitted through the film plus the substrate to the complex field amplitude $(\tilde{E}_s(\omega))$ transmitted only through the sapphire substrate (without the VO_2 layer) varies inversely with the complex frequency-dependent optical conductivity $(\tilde{\sigma}(\omega))$ using the expression[30–32]

$$\frac{\tilde{E}_{f+s}(\omega)}{\tilde{E}_s(\omega)} = \frac{1+n_s}{1+n_s+z_o\tilde{\sigma}(\omega)t_f}, \qquad (2)$$

where ω is the angular frequency, t_f is the film thickness ($t_f \sim 150$ nm), z_0 is the free space impedance, and n_s (~3.0) is the refractive index of the sapphire substrate. The THz amplitude ratio $|\tilde{E}_{f+s}(\omega)/\tilde{E}_s(\omega)|$ can be simulated using Eq. (2) and assuming the VO_2 conductivity is approximated by the DC (real part) σ_r^{DC}, taken as the reciprocal of the measured resistivity in Fig. 1. Figure 3 shows simulated $|\tilde{E}_{f+s}(\omega)/\tilde{E}_s(\omega)|$ as a function of temperature for the three investigated W-doped VO_2 samples. Good agreement between simulations and experiment is evident from Fig. 3.

The frequency-dependent real $(\sigma_r(\omega))$ and imaginary $(\sigma_i(\omega))$ components of the complex optical conductivity of W-doped VO_2 films can be determined by solving Eq. (2). In this case, both amplitude and phase of the ratio $\tilde{E}_{f+s}(\omega)/\tilde{E}_s(\omega)$ were taken into consideration. Figure 4(a) shows

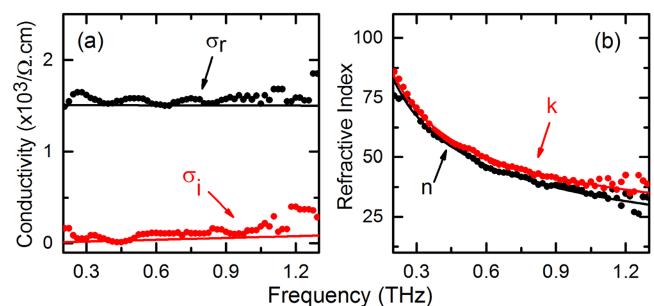

FIG. 4. (a) THz frequency-dependent complex optical conductivity and (b) refractive index in the metallic state (T = 80 °C) for sample S3.

representative $\sigma_r(\omega)$ and $\sigma_i(\omega)$ in the metallic phase for samples S3 at T = 80 °C. As shown in Fig. 4(a), $\sigma_r(\omega)$ and $\sigma_i(\omega)$ do not change significantly over the investigated THz frequency range. For samples S0, S1, S2, and S3, we determined average σ_r values of $\sim 2.4 \times 10^3$, $\sim 1.5 \times 10^3$, $\sim 1.7 \times 10^3$, and $\sim 1.5 \times 10^3 \Omega^{-1}$ cm^{-1}, respectively, in the metallic phase. These values are in good agreement with conductivities obtained from the DC resistivity measurements.

The complex conductivity of W-doped VO_2 films in the metallic phase can be described by the Drude model.[7] We determined the plasma frequency (ω_p) and the momentum relaxation time (τ) of the investigated samples by fitting the complex conductivity obtained in Fig. 4(a) with the Drude expression[30–32]

$$\tilde{\sigma}(\omega) = \frac{\varepsilon_o \omega_p^2 \tau}{1 - i\omega\tau}, \quad (3)$$

where, ε_0 is the vacuum permittivity. The fitting results are also shown in Fig. 4(a). From the fittings, we determined $\omega_p = 1569$, 1023, 1212, and 933 rad THz and $\tau = 11$, 14, 11, and 18 fs for samples S0, S1, S2, and S3, respectively.

The real ($n(\omega)$) and imaginary ($\kappa(\omega)$) parts of the complex refractive index ($\tilde{n}(\omega)$) can now be determined from the relation between the complex dielectric constant ($\tilde{\varepsilon}(\omega)$) and the complex conductivity ($\tilde{\sigma}(\omega)$) through the expression[31]

$$\tilde{\varepsilon}(\omega) = [\tilde{n}(\omega)]^2 = [n(\omega) + i\kappa(\omega)]^2 = 1 + i\frac{\tilde{\sigma}(\omega)}{\omega\varepsilon_o}. \quad (4)$$

Using the results shown in Fig. 4(a), we determined the frequency-dependent real and imaginary parts of the complex refractive index (in the metallic phase), $n(\omega)$, and $\kappa(\omega)$, respectively. Figure 4(b) shows the results for sample S3. Similar to undoped VO_2 films, the large dependence of n and κ with frequency is characteristic of the metallic behavior of both films at high temperatures.[6] The refractive indexes of samples S1 and S2 (not shown here) are essentially identical to that shown for sample S3 since all three samples have comparable resistivities for $T \gg T_{MIT}$ (see Fig. 1).

As mentioned earlier, THz analog modulation applications would require VO_2 based devices with broad phase transition temperature widths and low T_{MIT} to allow precise control of the optical properties *within* the MIT. The results shown in Figs. 1 and 3 suggest that W-doped VO_2 films with characteristics similar to that of sample S3 meet these requirements. To verify this premise, we show, in Fig. 5, the temperature dependence of the real and imaginary parts of the refractive index (at f = 0.5 THz) during heating and cooling cycles for sample S3. Both real and imaginary parts of the refractive index varied from ~20 to 50 when the temperature ranged from 35 to 80 °C. The striking feature of Fig. 5 is the large variation of both n and κ over a wide range of temperatures when compared to the abrupt phase transitions typically observed for undoped VO_2 films. This further confirms the potential of W-doped VO_2 films to realize analog devices operating at THz frequencies.

In summary, we have studied the temperature dependence of THz transmission properties for W-doped VO_2/sapphire with varying tungsten content. Our results reveal that the incorporation of W into the VO_2 significantly alters the

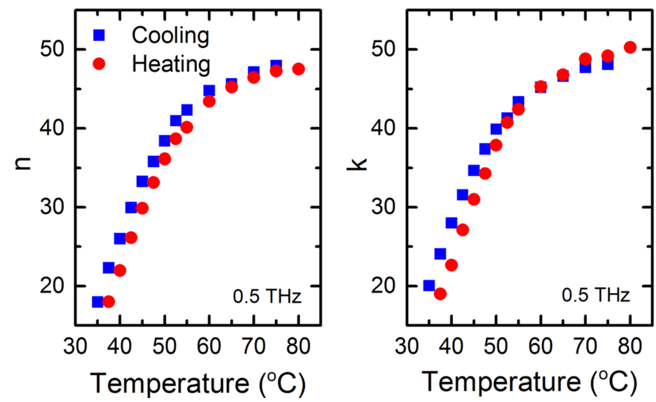

FIG. 5. Temperature dependent THz refractive index for sample S3 during heating and cooling cycles at f = 0.5 THz.

THz optical properties of the investigated samples. THz optical characteristics of W-doped VO_2 films were determined and the results are found to correlate with the temperature dependence of the electrical resistivity of the same samples across the phase transition. Characteristic metal-insulator temperature and phase transition width of ~40 and 35 °C, respectively, were determined for the doped VO_2 sample with the highest W content. We show that the refractive index of W-doped VO_2 can exhibit large variations and can be continuously tuned. This tuning facilitates precise control of the transmission properties of the VO_2 films to realize future active THz optical devices for analog applications.

The authors acknowledge support for this work from NSF (ECCS 1128644).

[1]J. Rozen, R. Lopez, R. F. Haglund, Jr., and L. C. Feldman, Appl. Phys. Lett. **88**, 081902 (2006).
[2]J. Lappalainen, S. Heinilehto, S. Saukko, V. Lantto, and H. Jantunen, Sens. Actuators, A **142**, 250 (2008).
[3]S. Chen, H. Ma, X. Yi, T. Xiong, H. Wang, and C. Ke, Sens. Actuators, A **115**, 28 (2004).
[4]S. B. Choi, J. S. Kyoung, H. S. Kim, H. R. Park, D. J. Park, B.-J. Kim, Y. H. Ahn, F. Rotermund, H.-T. Kim, and K. J. Ahn, Appl. Phys. Lett. **98**, 071105 (2011).
[5]M. D. Goldflam, T. Driscoll, B. Chapler, O. Khatib, N. Marie Jokerst, S. Palit, D. R. Smith, B.-J. Kim, G. Seo, and H.-T. Kim, Appl. Phys. Lett. **99**, 044103 (2011).
[6]Y. Zhu, Y. Zhao, M. Holtz, Z. Fan, and A. A. Bernussi, J. Opt. Soc. Am. B **29**, 2373 (2012).
[7]Q.-Y. Wen, H.-W. Zhang, Q.-H. Yang, Y.-S. Xie, K. Chen, and Y.-L. Liu, Appl. Phys. Lett. **97**, 021111 (2010).
[8]Y.-G. Jeong, H. Bernien, J.-S. Kyoung, H.-R. Park, H. S. Kim, J.-W. Choi, B.-J. Kim, H.-T. Kim, K. J. Ahn, and D.-S. Kim, Opt. Express **19**, 21211 (2011).
[9]J. S. Kyoung, M. A. Seo, S. M. Koo, H. R. Park, H. S. Kim, B. J. Kim, H. T. Kim, N. K. Park, D. S. Kim, and K. J. Ahn, Phys. Status Solidi C **8**, 1227 (2011).
[10]S. Lysenko, V. Vikhnin, F. Fernandez, A. Rua, and H. Liu, Phys. Rev. B: Condens. Matter **75**, 075109 (2007).
[11]J. V. Ryckman, J. Nag, R. E. Marvel, B. K. Choi, R. F. Haglund, and S. M. Weiss, Opt. Express **20**, 13215 (2012).
[12]M. A. Sobhan, R. T. Kivaisi, B. A. Stjerna, and C.-G. Granqvist, in "Reactively sputtered thermochromic tungsten-doped VO_2 films," Proc. SPIE **2255**, 423 (1994).
[13]B. G. Chae, H. T. Kim, and S. J. Yun, Electrochem. Solid-State Lett. **11**, D53 (2008).
[14]T. D. Manning, I. P. Parkin, M. E. Pemble, D. Sheel, and D. Vernardou, Chem. Mater. **16**, 744 (2004).
[15]A. Romanyuk, R. Steiner, L. Marot, and P. Oelhafen, Sol. Energy Mater. Sol. Cells **91**, 1831 (2007).

[16]P. Jin and S. Tanemura, Jpn. J. Appl. Phys., Part 1 **34**, 2459 (1995).
[17]C. Si, W. Xu, H. Wang, J. Zhou, A. Ablat, L. Zhang, J. Cheng, Z. Pan, L. Fan, and C. Zou, Phys. Chem. Chem. Phys. **14**, 15021 (2012).
[18]M. Mao, W.-X. Huang, Y.-X. Zhang, J.-Z. Yan, Y. Luo, Q.-W. Shi, and J.-H. Cai, J. Inorg. Mater. **27**, 891 (2012).
[19]D. Vernardou, M. E. Pemble, and D. W. Sheel, Chem. Vap. Deposition **13**, 158 (2007).
[20]W. Xue-Jin, L. Yu-Ying, L. De-Hua, F. Bao-Hua, H. Zhi-Wei, and Q. Zheng, Chin. Phys. B **22**, 066803 (2013).
[21]C. Tang, P. Georgopoulos, M. E. Fine, J. B. Cohen, M. Nygren, G. S. Knapp, and A. Aldred, Phys. Rev. B: Condens. Matter **31**, 1000 (1985).
[22]S. Lu, L. Hou, and F. Gan, J. Mater. Sci. Lett. **15**, 856 (1996).
[23]S. Xu, H. Ma, S. Dai, and Z. Jiang, J. Mater. Sci **39**, 489 (2004).
[24]C. Piccirillo, R. Binions, and I. P. Parkin, Eur. J. Inorg. Chem. **2007**, 4050.
[25]T. E. Phillips, R. A. Murphy, and T. O. Poehler, Mater. Res. Bull. **22**, 1113 (1987).
[26]J. Du, Y. Gao, H. Luo, L. Kang, Z. Zhang, Z. Chen, and C. Cao, Sol. Energy Mater. Sol. Cells **95**, 469 (2011).
[27]Y. Zhao, J. H. Lee, Y. Zhu, M. Nazari, C. Chen, H. Wang, A. Bernussi, M. Holtz, and Z. Fan, J. Appl. Phys. **111**, 053533 (2012).
[28]T. Ben-Messaoud, G. Landry, J. P. Gariépy, B. Ramamoorthy, P. V. Ashrit, and A. Haché, Opt. Commun. **281**, 6024 (2008).
[29]H. Wang, X. Yi, and Y. Li, Opt. Commun. **256**, 305 (2005).
[30]M. Walther, D. G. Cooke, C. Sherstan, M. Hajar, M. R. Freeman, and F. A. Hegmann, Phys. Rev. B: Condens. Matter **76**, 125408 (2007).
[31]G. Ma, D. Li, H. Ma, J. Shen, C. Wu, J. Ge, S. Hu, and N. Dai, Appl. Phys. Lett. **93**, 211101 (2008).
[32]A. Thoman, A. Kern, H. Helm, and M. Walther, Phys. Rev. B: Condens. Matter **77**, 195405 (2008).